Executive Summary of the Thesis

Growth of iron phthtalocyanine molecules on Cr_2O_3/Cu(110)

Laurea Magistrale in Engineering Physics - Ingegneria Fisica

Author: Matteo Panzeri

Advisor: Prof. Andrea Picone

Co-advisor: Prof. Alberto Brambilla

Academic year: 2021-2022

1. Introduction

The field of Spintronics, also known as spin-electronics, aims at detecting the response of electron spins to an external stimulus and implementing such response into novel devices with logic, sensing, and memory capabilities. The majority of studies on Spintronics have focused on inorganic semiconductors and ferromagnetic layers. In recent years, however, attention has been driven to other classes of materials, among which organic semiconductors (OSCs) have shown very interesting properties. The main advantage of OSCs for spintronic applications is the long spin relaxation time of carriers that results from the small spin-orbit coupling [1]. Organic semiconductors are usually small molecules or π-conjugated polymers and they usually possess weak spin-orbit coupling since they are mostly composed of light materials such as carbon, oxygen, and hydrogen. Moreover, when organic molecules are brought together with a magnetic layer, new hybrid electronic states form at the interface. The DOS of the molecules gets modified in two ways: first, the lifetime of each molecular orbital becomes finite, enabling electrons to leak in and out of the molecule and broadening its DOS, second, the molecules' energy levels can be shifted. Both the

shift and the broadening can be spin-dependent, so that the spin-polarization of the current can be very different, or even opposite in sign, from that of the electrodes, depending on which spin-polarized molecular orbital can end up at E_F and thus dominate the current. This possibility of tailoring the spin-polarization of a certain interface with suitable organic materials gave rise to a new branch of Spintronics which has been dubbed *spinterface science* [2].

Another promising field of Spintronics is that of antiferromagnetic Spintronics. As the name suggests, this field deals with antiferromagnets. Antiferromagnets (AFs) are magnetically ordered, but the neighbouring magnetic moments point in opposite directions, thus resulting in zero net magnetization: this means that antiferromagnets do not produce stray fields and they are insensitive to external magnetic field perturbations [3]. These characteristics make AFs promising candidates for applications in magnetic memory elements, which can be more closely packed, leading to higher storage density. A key difference is found in the dynamics of antiferromagnets and ferromagnets. Even though it is possible to depict an antiferromagnet as two interpenetrating ferromagnets, the intersublattice exchange makes the dynamics of AFs richer than that of FMs. In particular, the

collective spin-torque oscillations (also known as *spin waves*) of AFs fall in the THz regime [3], and they can be excited not only by purely electric signals, but also by magnetic THz pulses and by ultrafast optical pump systems, which makes AFs attractive for data storage and processing applications [4].

These new perspectives of Spintronics provide the background that motivated this thesis work. The aim of this thesis is to study the growth of a molecular layer of iron phthalocyanines (FePcs), as a candidate for an organic layer with semiconducting properties [5], on top of antiferromagnetic Cr_2O_3 on Cu(110). The thesis work is divided into two parts: first, the growth and crystallographic properties of Cr_2O_3 grown on Cu(110) and Cu(111) have been investigated; then, the structural and magnetic properties of FePc grown on Cr_2O_3/Cu(110) have been characterized.

2.   Experimental Methods

The majority of the measurements presented in this work were performed at the STM Laboratory, located in the Physics Department at Politecnico di Milano. The experimental setup consists of two Ultra High Vacuum (UHV) chambers. One chamber is dedicated to the *in situ* preparation of the samples. Cu(110) and Cu(111) single crystal substrates were prepared via repeated cycles of Ar^+ ion sputtering ($I = 15$ μA, $V = 1.5$ keV) and thermal annealing at $T = 480°$ C. Chromium oxide and iron phthalocyanine films were grown via Molecular Beam Epitaxy (MBE), and the deposition rates were calibrated with a quartz microbalance. Both the chemical characterization through Auger Electron Spectroscopy (AES) and the crystallographic characterization of the samples through Low Energy Electron Diffraction (LEED) were performed in this first UHV chamber. The experimental setup for AES and LEED is the same, and it is composed of an electron gun, a multi-grid system that has the purpose of selecting only the elastically scattered electrons, a set of focusing lenses, and a fluorescent screen that is kept at a high voltage (around 5 kV) to accelerate the electrons and stimulate fluorescent emission. Electrons are emitted by thermionic effect from a LaB_6 filament. A Wehnelt electrode is kept at a negative potential with respect to the filament to favour the extraction of electrons. The typical energies employed for LEED measurements range from 25 to 200 eV. Images were acquired with a CCD camera. In the case of AES, the differential signal dN/dE, where $N(E)$ is the number of electrons at a certain energy E, was acquired. The second chamber is dedicated to the morphological characterization of the surface via Scanning Tunneling Microscopy (STM). STM measurements were performed ar RT in constant-current mode, which, as the name suggests, consists in maintaining a constant tunneling current during the scan by adjusting the sample-tip distance. The bias voltage is reported in each measurement and it is referred to the sample. The tunneling current signal is detected by the electronic components and it is then processed via software (*Matrix* in this case) to obtain the image. The other spectroscopic techniques present in this work, namely X-Ray Absorption Spectroscopy (XAS) and X-Ray Magnetic Circular Dichroism (XMCD), were performed at APE-HE beamline located in Elettra synchrotron facility in Trieste.

3.   Results

3.1.   Oxide growth

Chromium oxide growth was characterized on two different substrates, Cu(110) and Cu(111). The growth of oxide thin films was performed by reactive deposition at $T = 435°$ C in oxygen environment at pressure $p_{O_2} = 10^{-6}$ mbar, followed by annealing at the same temperature and oxygen pressure for $\Delta t = 1'$. AES was used to check the chemical composition and thickness of Cr_2O_3. The stages of Cr_2O_3 growth are reported in Figure 1. For coverage of 0.3 nm (Figure 1(a)), the oxide appears to form atomically flat islands with a constant height of 1 nm, which corresponds to a single Cr_2O_3 cell. Upon increasing the coverage to 0.45 (Figure 1(b)) nm and then to 0.6 nm (Figure 1(c)), the islands become larger but at the same time a new layer with a thickness of 0.5 nm starts to form. Despite the formation of this second layer, the enlargement of the islands suggests the possibility of saturating the surface for higher coverage. In fact, by increasing the coverage to 1.2 nm. the surface appears to be totally covered by the
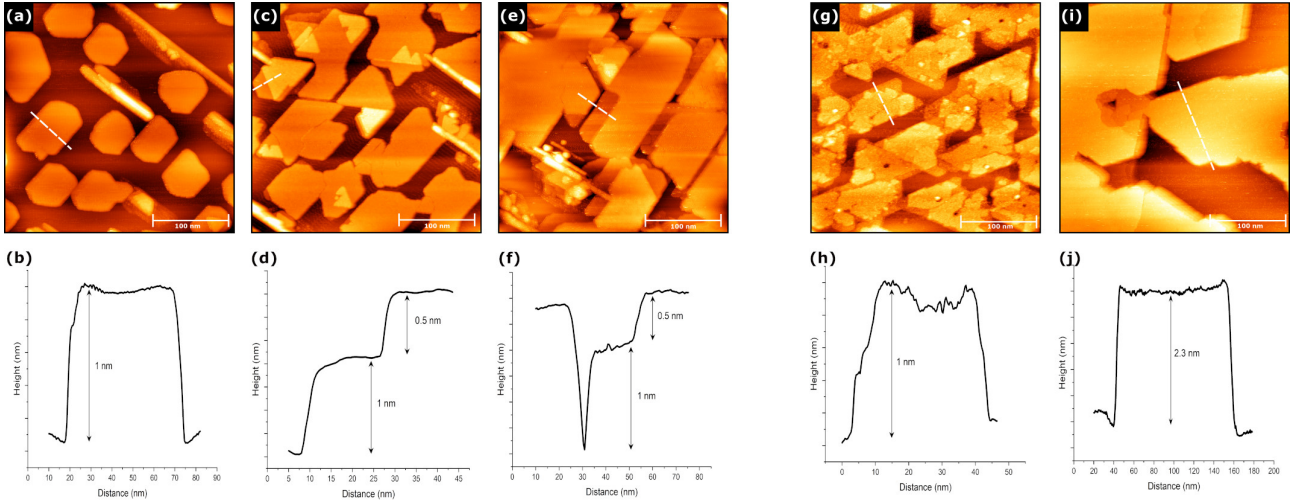
Figure 1: STM images (300×300 nm^2) of Cr_2O_3 (a) 0.3 nm thickness on Cu(110) with topographical curve (b) corresponding to white line, $\Delta V = -2$ V, $I = 0.5$ nA; (c) 0.45 nm on Cu(110) with topographical curve (d), $\Delta V = -1.8$ V, $I = 0.5$ nA; (e) 0.6 nm on Cu(110) with topographical curve (f), $\Delta V = -2$ V, $I = 0.5$ nA; (g) 0.6 nm on Cu(111) with topographical curve (h), $\Delta V = -1.8$ V, $I = 0.4$ nA; (i) 1.2 nm on Cu(111) with topographical curve (j), $\Delta V = -3.3$ V, $I = 0.2$ nA

oxide. However, the sample becomes too insulating to obtain a good STM image. The oxide growth on Cu(111) for 0.6 nm, represented in Figure 1(d), appears similar to the one on Cu(110) for the same coverage, with 1 nm high islands and a second layer that is forming on top of them. However, for higher coverage, the islands do not seem to merge anymore, but they seem to grow higher. As depicted in Figure 1(e), islands with heights of 2-2.5 nm have been observed, and they are separated by wide areas of bare Cu. Given the impossibility to saturate the surface, it has been decided to grow the FePc molecular layer only on Cr_2O_3/Cu(110). The LEED patterns have been taken to check the crystallographic quality of the oxides. Figure 2

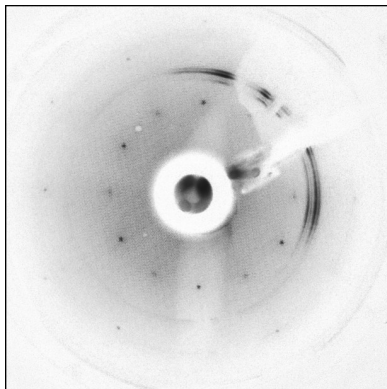shows the LEED pattern of Cr_2O_3/Cu(110), which consists of two hexagonal patterns rotated by 30°. This suggests the presence of two rotated hexagonal domains, one of which appears to be more long-range ordered than the other, because there is one hexagonal pattern that is brighter than the other. The elongated islands that are visible in Figure 1(a) are likely responsible for the less intense LEED domain. The LEED of Cr_2O_3/Cu(111), represented in Figure 5, shows, on the other hand, a single hexagonal pattern. It is possible to observe double spots: the inner ones are related to the oxide, while the outer ones belong to the substrate, which also has a hexagonal LEED pattern. A further characterization concerns the stoichiom-
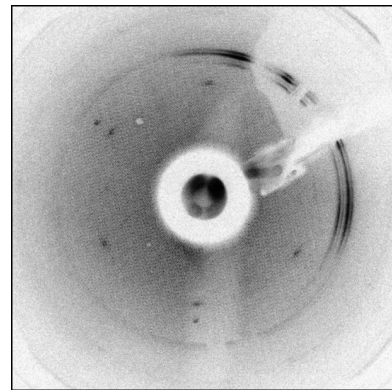

Figure 2: LEED of Cr_2O_3/Cu(110), 200 eV

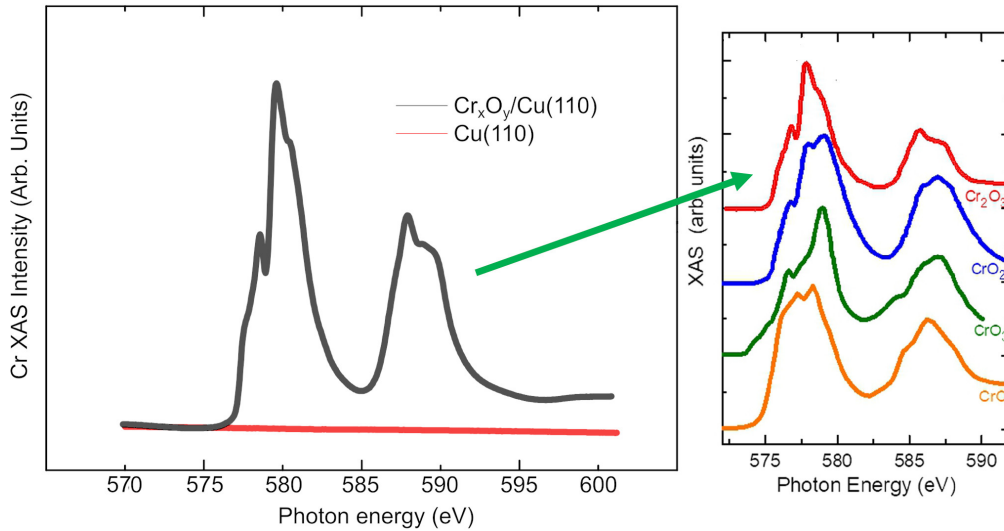Figure 5: LEED of Cr_2O_3/Cu(111), 200 eV
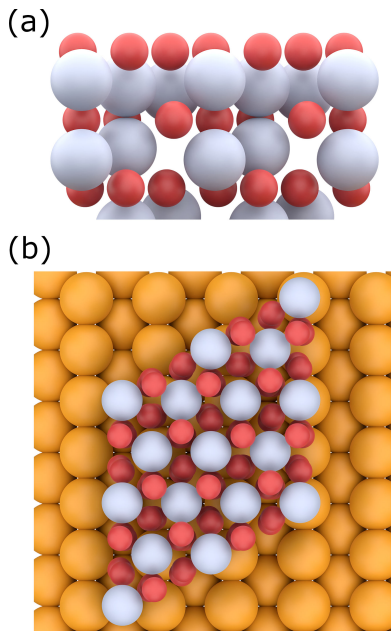
3

Figure 3: $L_{2,3}$ edge XAS of Cr_2O_3

Figure 4: (a) side view of CrO reconstruction; (b) top view of hexagonal chromium oxide surface

etry of the oxide. The measurement of X-Ray Absorption Spectroscopy (XAS) was taken on $Cr_2O_3/Cu(110)$ to check if the oxide grown on the substrate has the correct stoichiometry. The XAS at the $L_{2,3}$ edges is reported in Figure 3, alongside with some reference XAS spectra of CrO, CrO_2, CrO_3 taken from litterature [6]. The similarity of the experimental XAS spectrum with the reference spectrum of Cr_2O_3 is evident and it confirms that Cr atoms are in a +3 oxidation state, therefore the chromium ox-

ide film grown on Cu(110) is indeed Cr_2O_3. The other spectra corresponding to different oxidation states of Cr can be easily ruled out. The lattice parameter of grown Cr_2O_3 can be estimated from LEED pattern and it is found to be 2.95 Å, which is rather distant from the 4.96 Å of bulk-terminated $Cr_2O_3(0001)$ surface. A possible solution is that Cr_2O_3 undergoes a CrO surface reconstruction. The CrO reconstruction, as represented in Figure 4 can be thought of as a bulk-terminated Cr_2O_3, in which the Cr hexagons intercalated below the oxygen. With this surface reconstruction, the hexagonal structure is retrieved.

3.2. FePc film growth

The deposition of FePc was performed via MBE at room temperature. The first STM image reported in Figure 6(a), is related to a sub-monolayer coverage. Here the molecules appear to be ordered on the chromium oxide island in a hexagonal arrangement with a periodicity of 1.5 nm. The second image (Figure 6(b)) shows a full monolayer coverage of FePc. In this figure, it is possible to distinguish the ordered layer on top of the metal, while the molecules on the oxide appear to be rather disordered. There are small regions on the oxide in which a short-range order of the molecules appears; this suggests annealing the sample to increase the mobility of the molecules and possibly obtain some longer-range order. Even in this case, however, it was never possible to observe an ordered layer. Nev-
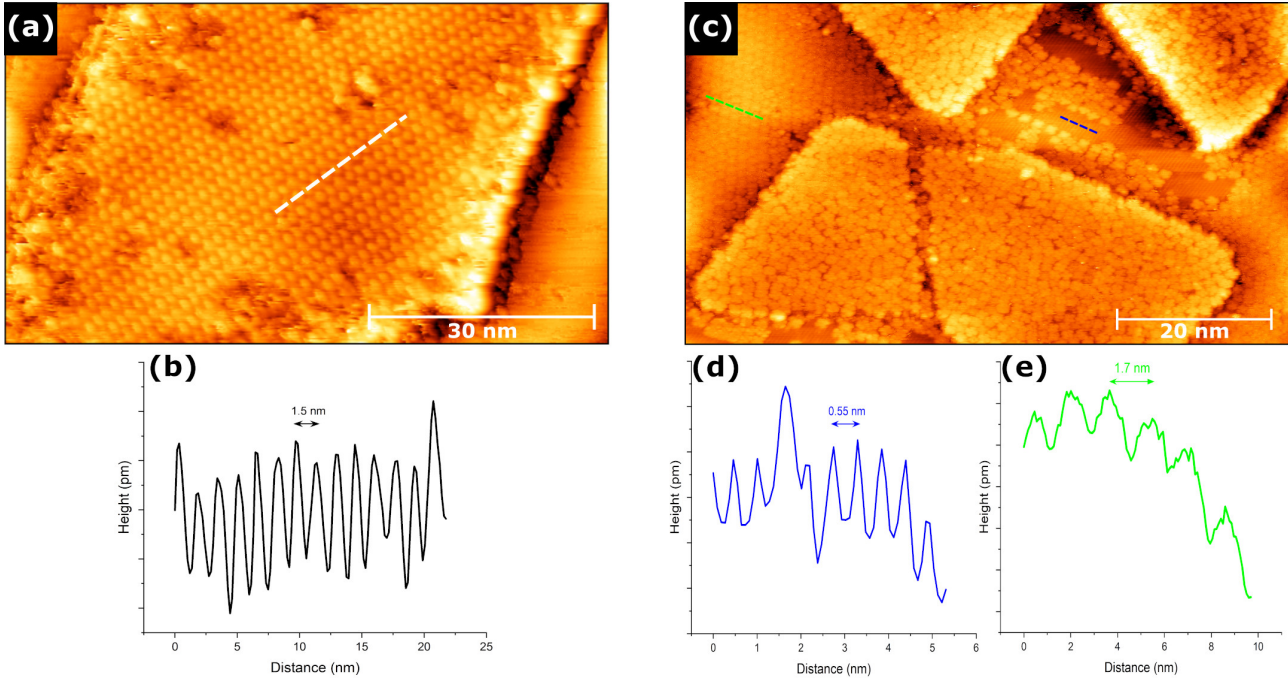
Figure 6: STM images of FePc/Cr$_2$O$_3$/Cu(110) (a) sub-monolayer coverage with topographical curve (b) corresponding to white line, 80×45 nm^2, $\Delta V = -1.8$ V, $I = 0.6$ nA; (c) full monolayer coverage with topographical curve corresponding to blue line (d) and green line (e), 90×60 nm^2, $\Delta V = -2$ V, $I = 0.6$ nA.

ertheless, the molecules lie on top of the oxide with planar geometry. This fact indicates that in this system the interaction between the oxide and the molecular overlayer is rather strong: this is a non-trivial result since the interaction between molecules and oxides is usually quite weak. A small periodicity of 0.55 nm is visible on the metal, and it is due to the p(2×1) surface reconstruction of oxygen on Cu: this reconstruction is formed during the reactive deposition of chromium oxide, when the Cu substrate is heated at $T = 435°$ C and it is exposed to oxygen at pressure $p_{O_2} = 10^{-6}$ mbar.

The XMCD measurement was taken on the L-edge of Fe and it was performed at 100 K. As depicted in Figure 7, the circular left (CL) and circular right (CR) XAS of Fe L-edge show differences both in shape and intensity. A non-zero dichroic signal is then retrieved from the subtraction of the two absorption spectra of the central Fe atom of iron phthalocyanines, revealing that a spin-polarization has been induced in the Fe^{2+} $2p$ states, and it is indicative of ferromagnetic ordering. A possible explanation for this magnetic polarization of Fe^{2+} states can be found in the coupling of the molecular overlayer with the last layer of Cr$_2$O$_3$. The Cr$_2$O$_3$(0001)

is, in fact, a non-magnetically compensated surface. In the chromium oxide structure, each Cr layer is magnetically compensated by the upper one, because of the antiferromagnetic coupling. Thus, the surface layer remains uncompensated: the Fe^{2+} ions of the molecular overlayer are coupled to the topmost layer of chromium oxide, and this results in the ferromagnetic ordering observed with XMCD.
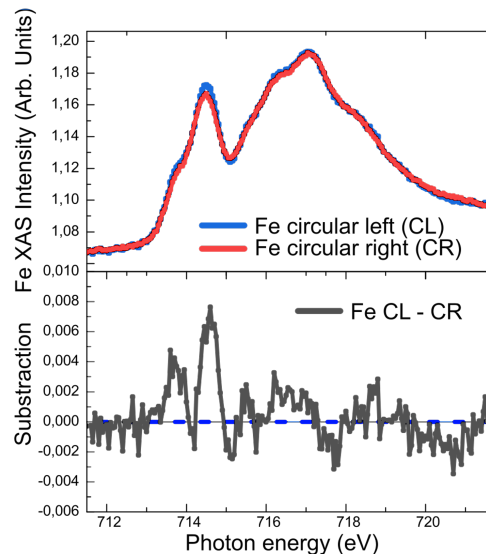

Figure 7: XMCD of FePc/Cr$_2$O$_3$/Cu(110)

4. Conclusions

In conclusion, the growth of iron phthalocyanine film has been performed on Cr_2O_3/Cu(110). The oxide growth has been characterized first on two different substrates, Cu(110) and Cu(111). The oxide growth is non-optimal in both cases, because the oxide tends to grow in islands instead of layer by layer. Scanning Tunneling Microscopy (STM) measurements have shown that while the islands of Cr_2O_3/Cu(110) tend to remain at the same height and become larger as the coverage increases, in the case of Cr_2O_3/Cu(111) the islands become higher, up to 2-2.5 nm. For this reason, the FePc film was not grown on Cr_2O_3/Cu(111). Low Energy Electron Diffraction (LEED) has revealed that in both cases the oxide is crystalline, and in particular, the lattice estimation for Cr_2O_3/Cu(110) shows that the oxide undergoes a CrO surface reconstruction. The X-Ray Absorption Spectroscopy (XAS) measurement for Cr_2O_3/Cu(110) has shown that the oxide grows with the correct stoichiometry.

The FePc film was grown on Cr_2O_3/Cu(110). Despite the non-optimal surface morphology of the oxide, the STM measurements have revealed that the molecules grow on top of the oxide with a planar geometry. This highlights a rather strong interaction between the FePcs and the chromium oxide layer, a fact that is not trivial because the interaction of molecules with oxides is usually weak. However, while it was possible to observe the formation of an ordered layer for coverage below a monolayer, no long-range order was observed for full monolayer coverage. The magnetic properties of the organic layer have been investigated through X-Ray Magnetic Circular Dichroism (XMCD). The results demonstrated that the magnetic interaction between the chromium oxide surface and the molecular overlayer induces a spin-polarization in the Fe^{2+} $2p$ states, resulting in the ferromagnetic ordering of the molecular layer.

References

[1] W J M Naber, S Faez, and W G van der Wiel. Organic spintronics. *Journal of Physics D: Applied Physics*, 40(12):R205–R228, jun 2007.

[2] Stefano Sanvito. The rise of spinterface science. *Nature Physics*, 6(8):562–564, 2010.

[3] O. Gomonay, T. Jungwirth, and J. Sinova. Concepts of antiferromagnetic spintronics. *physica status solidi (RRL) – Rapid Research Letters*, 11(4):1700022, 2017.

[4] Xiao-Xiao Zhang, Lizhong Li, Daniel Weber, Joshua Goldberger, Kin Fai Mak, and Jie Shan. Gate-tunable spin waves in antiferromagnetic atomic bilayers. *Nature Materials*, 19(8):838–842, 2020.

[5] Christian G. Claessens, Uwe Hahn, and Tomás Torres. Phthalocyanines: From outstanding electronic properties to emerging applications. *The Chemical Record*, 8(2):75–97, 2008.

[6] M. Asa, G. Vinai, J. L. Hart, C. Autieri, C. Rinaldi, P. Torelli, G. Panaccione, M. L. Taheri, S. Picozzi, and M. Cantoni. Interdiffusion-driven synthesis of tetragonal chromium (iii) oxide on BaTio$_3$. *Phys. Rev. Materials*, 2:033401, Mar 2018.